**Figures and figure legends**

**Supplementary Figure 1**

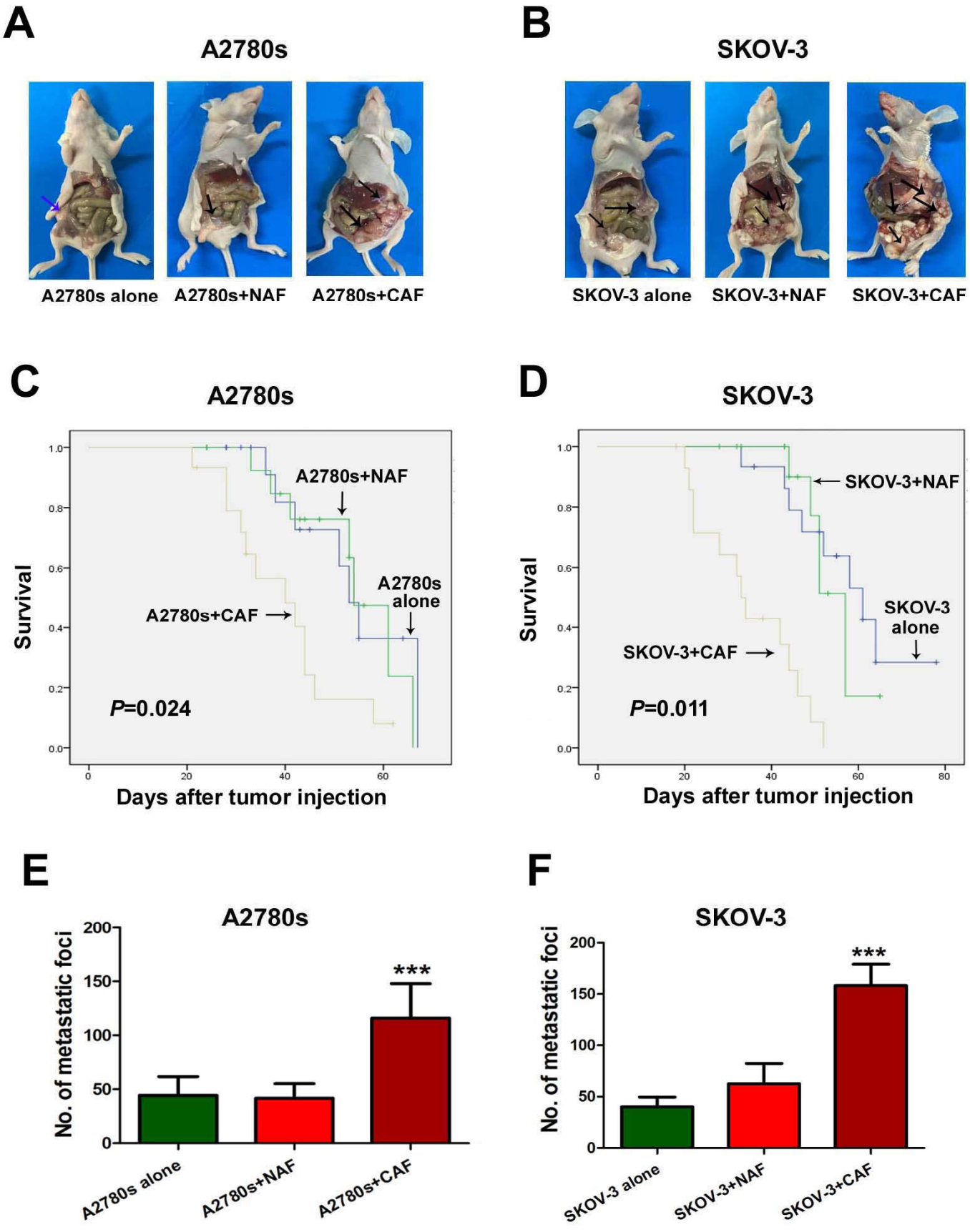

**Supplementary Figure 1. CAFs promote peritoneal metastasis of ovarian cancer.** (A) Representative pictures of peritoneal metastasis in an orthotopic model generated by intrabursal injection of A2780s cells alone or together with either CAFs or NAFs. (B) Representative pictures of peritoneal metastasis in an orthotopic model generated by intrabursal injection of SKOV-3 cells alone or together with either CAFs or NAFs. (C) Kaplan Meier analysis of mice inoculated with A2780s cells alone or together with either CAFs or NAFs. (D) Kaplan Meier analysis of mice inoculated with SKOV-3 cells alone or together with either CAFs or NAFs. (E) Number of metastatic nodules in abdominal cavity of mice inoculated with A2780s cells alone or together with either CAFs or NAFs. (F) Number of metastatic nodules in abdominal cavity of mice inoculated with SKOV-3 cells alone or together with either CAFs or NAFs. *, $P < 0.05$; **, $P < 0.01$; ***, $P < 0.001$.

**Supplementary Figure 2**

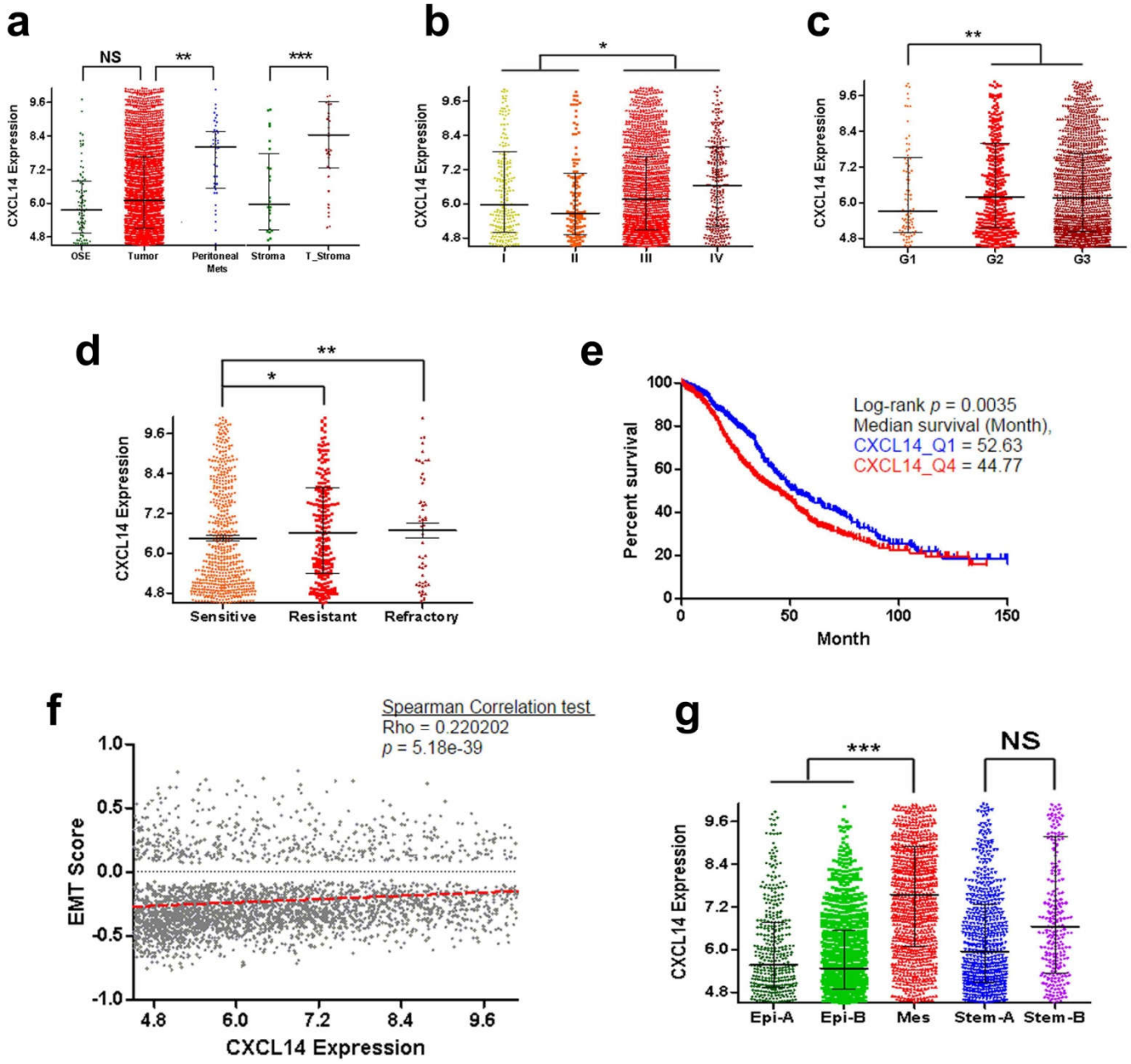


**Supplementary Figure 2. CSIOVDB analysis of CXCL14 expression in ovarian cancer.** (A) CXCL14 expression in normal ovary surface epithelium(OSE), ovarian tumor, peritoneal metastatic sites of ovarian cancer, stroma of normal ovary and stroma of ovarian cancer in CSIOVDB database. (B) CXCL14 expression in

specimens of ovarian cancer with different FIGO stages. (C) CXCL14 expression in specimens of ovarian cancer with different different differentiation grades (D) CXCL14 expression in specimens of chemotherapy-sensitive, resistant and refractory ovarian cancer. (E) Kaplan–Meier analysis of ovarian cancer patients in CSIOVDB database for the correlation between CXCL14 and overall survival. (F) Correlation between CXCL14 expression and epithelial-to-mesenchymal (EMT) scores in CSIOVDB database. (G) Expression of CXCL14 in different molecular subtypes of ovarian cancer in CSIOVDB database. *, $P < 0.05$; **, $P < 0.01$; ***, $P < 0.001$.

**Supplementary Figure 3**

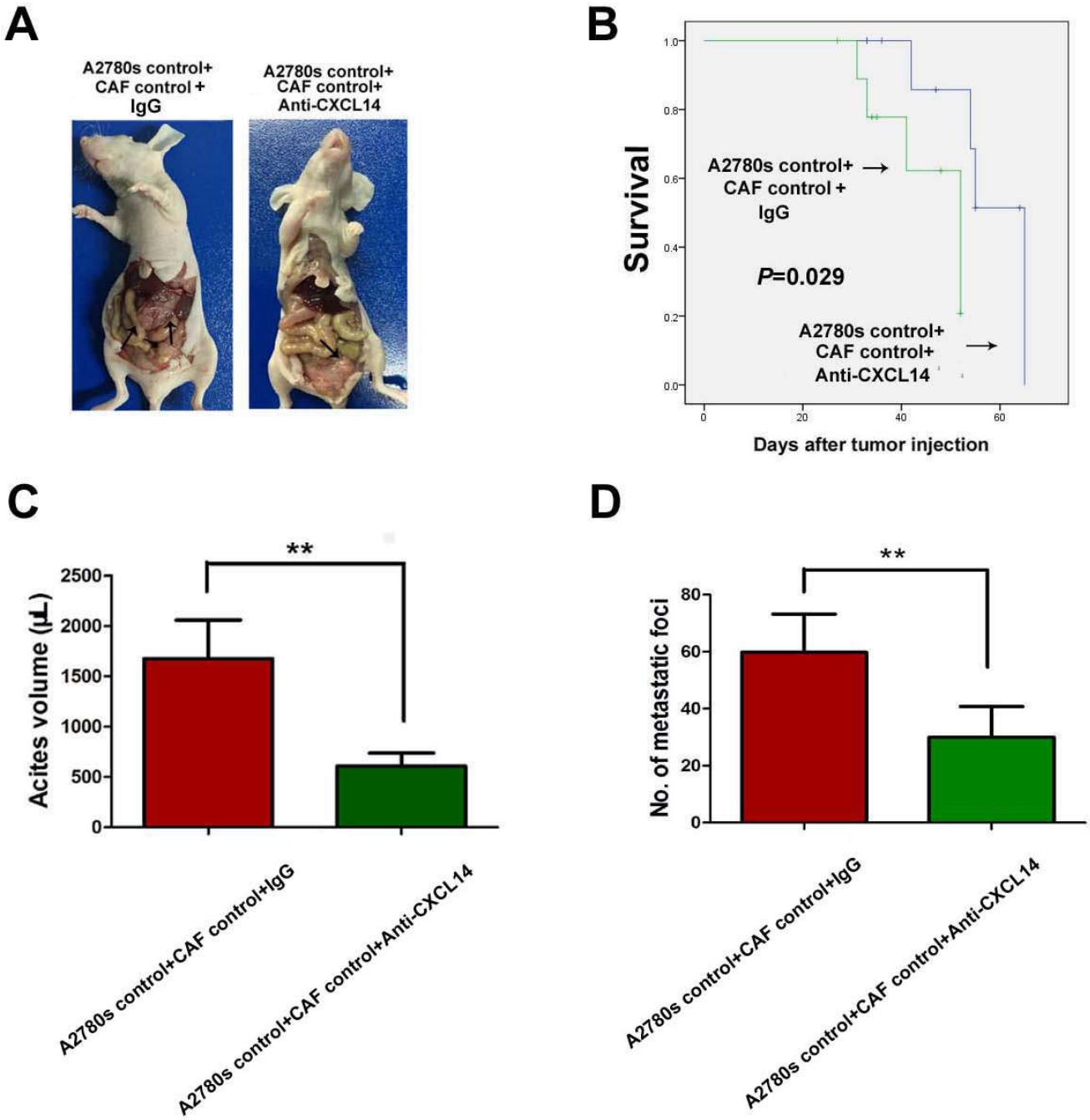

**Supplementary Figure 3. CXCL14 inhibition attenuates ovarian cancer metastasis in vivo.** (A) Representative pictures of peritoneal metastasis in an orthotopic model generated by intrabursal injection of a combination of A2780s cells and control CAFs treated with IgG or A2780s cells and control CAFs treated with anti-human CXCL14 antibody. Anti-human CXCL14 antibody or IgG were administered at 2 mg/kg twice weekly by i.p. injection. (B) Kaplan Meier analysis of mice inoculated with a combination of A2780s cells and control CAFs treated with IgG or A2780s cells and control CAFs treated with anti-CXCL14 antibody. (C) Box plot of ascites volume in abdominal cavity of mice inoculated with a combination of A2780s cells and control CAFs treated with IgG or A2780s cells and control CAFs treated with anti-CXCL14 antibody. (D) Box plot of number of metastatic nodules in abdominal cavity of mice inoculated with a combination of A2780s cells and control CAFs treated with IgG or A2780s cells and control CAFs treated with anti-CXCL14 antibody. *, $P < 0.05$; **, $P < 0.01$; ***, $P < 0.001$.

**Supplementary Figure 4**

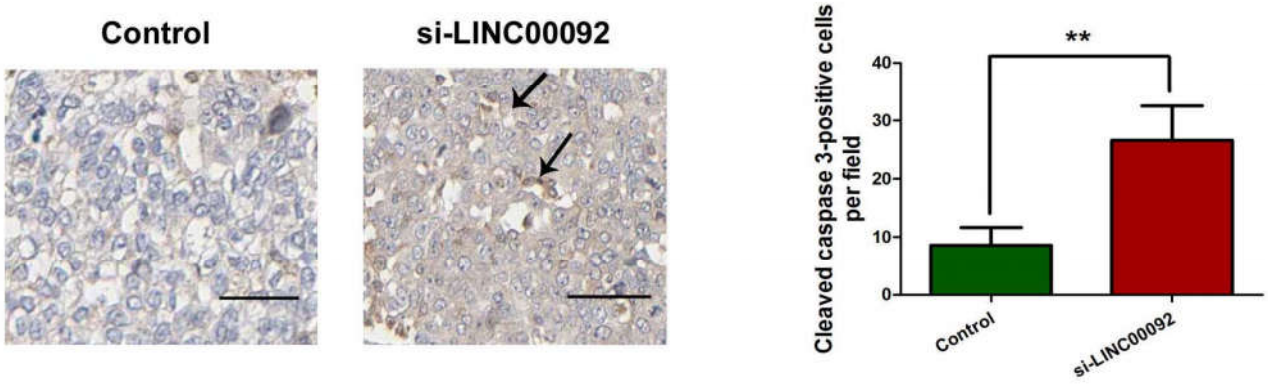


**Supplementary Figure 4. LINC00092 silencing induced increase of cleaved caspase-3 in specimens of ovarian cancer peritoneal metastasis model in nude mice.** *, $P < 0.05$; **, $P < 0.01$; ***, $P < 0.001$. Scale Bar=50μm.

**Supplementary Figure 5**

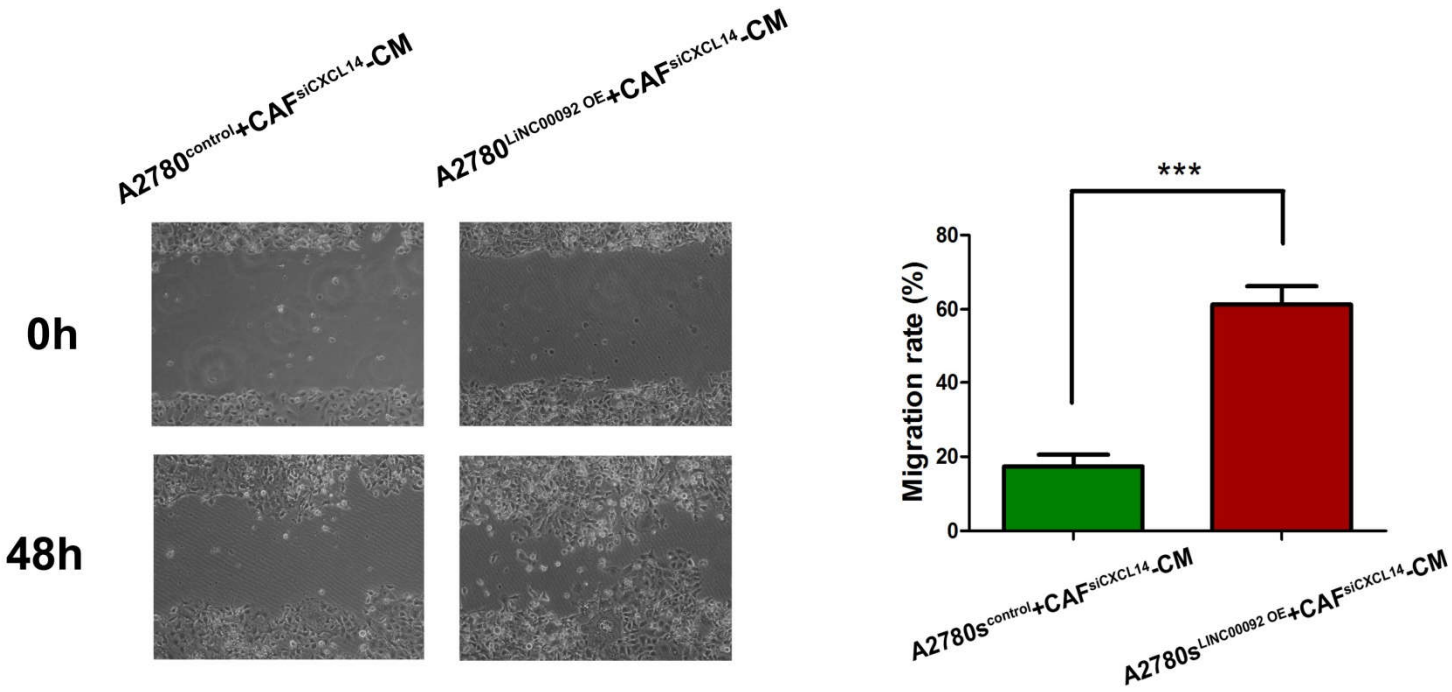


**Supplementary Figure 5. Enhanced LINC00092 expression in ovarian cancer cells could offset the metastasis-attenuating effects of CXCL14 knockdown in CAFs.** Wound healing analysis of A2780s cells or LINC00092-overexpressing A2780s cells cocultured with CM from CXCL14-knockdown CAFs. *, $P < 0.05$; **, $P < 0.01$; ***, $P < 0.001$.

**Supplementary Figure 6**

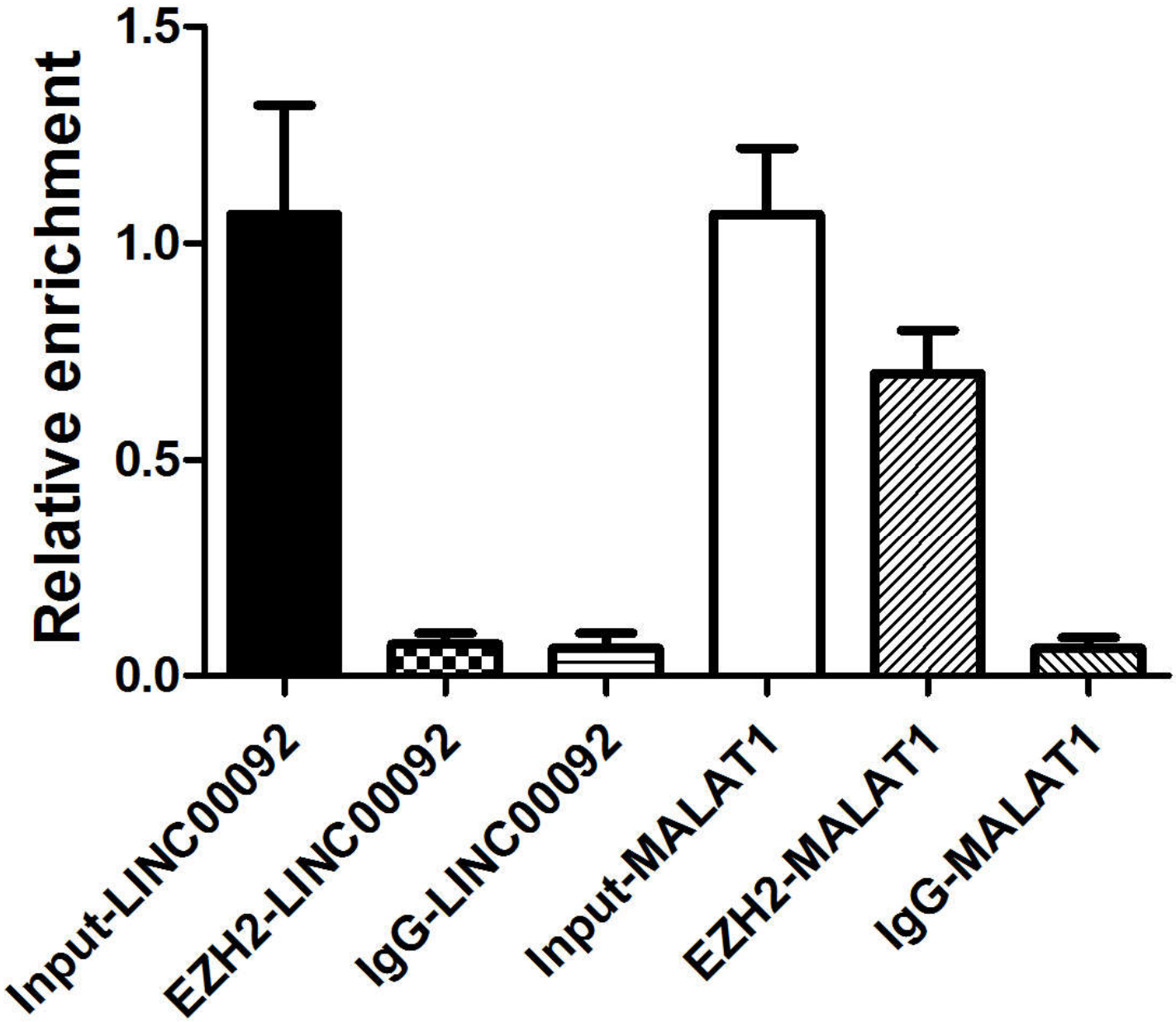


**Supplementary Figure 6. RIP experiments were performed using an antibody against EZH2 on extracts from A2780s cell line. MALAT1 was used as a positive control that physically associates with EZH2.**

**Supplementary Figure 7**

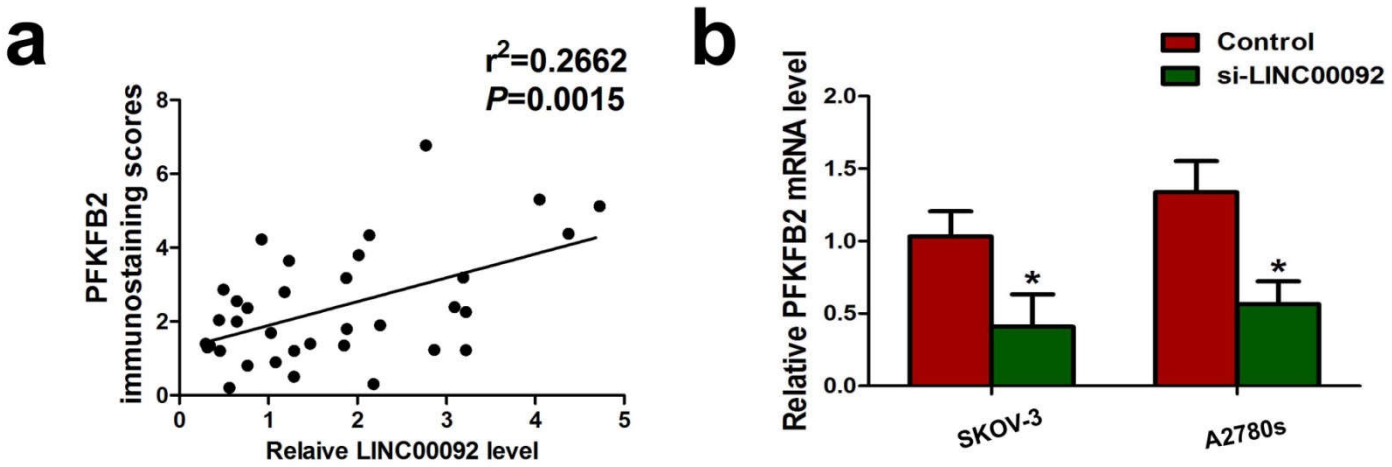


**Supplementary Figure 7. Correlation between LINC00092 level and PFKFB2 expression in ovarian cancer.** (A) Correlation between relative LINC00092 expression level and PFKFB2 immunostaining scores. (B) Relative PFKFB2 mRNA levels in ovarian cancer cell lines after LINC00092 knockdown. All experiments were performed in triplicate. *, $P < 0.05$; **, $P < 0.01$; ***, $P < 0.001$.

**Supplementary Figure 8**

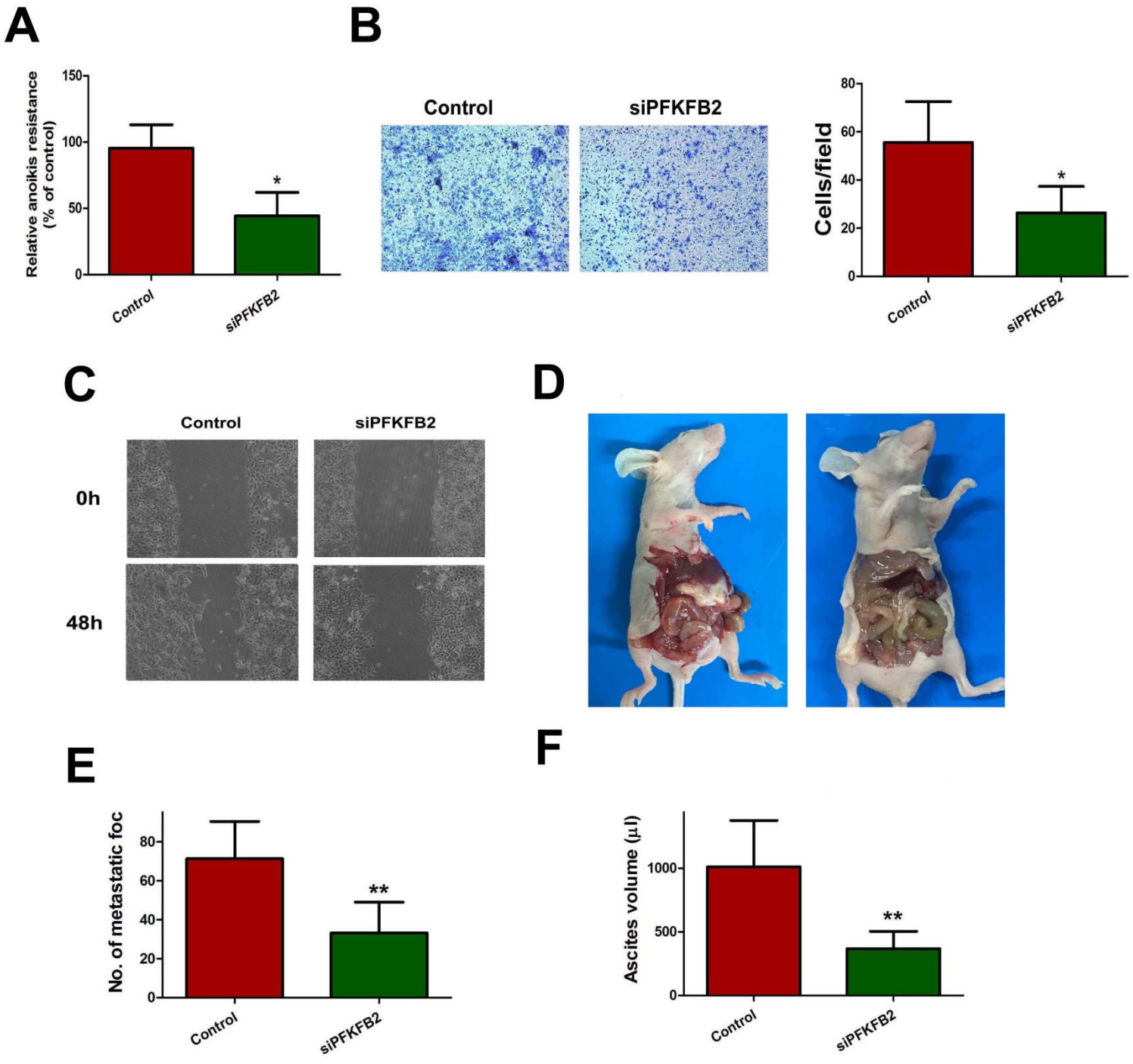


**Supplementary Figure 8. PFKFB2 in the maintenance of metastatic phenotype of ovarian cancer.** (A) Relative anoikis resistance rate in control A2780s cells and A2780s cells transfected with PFKFB2 siRNA. (B) Transwell assay for A2780s cells

transfected with control and PFKFB2 siRNA, respectively. (C) Wound healing analysis of A2780s cells transfected with control and PFKFB2 siRNA, respectively. (D) Representative pictures of peritoneal metastasis in mice inoculated with control A2780s cells and PFKFB2-silenced A2780s cells, respectively. (E) Box plot of number of metastatic nodules in the abdominal cavities of an orthotopic model generated by intrabursal injection of control A2780s cells and PFKFB2-silenced A2780s cells, respectively. (F) Box plot of the ascites volumes collected from the abdominal cavities of an orthotopic model generated by intrabursal injection of control A2780s cells and PFKFB2-silenced A2780s cells, respectively. *, $P < 0.05$; **, $P < 0.01$; ***, $P < 0.001$.

**Supplementary Figure 9**

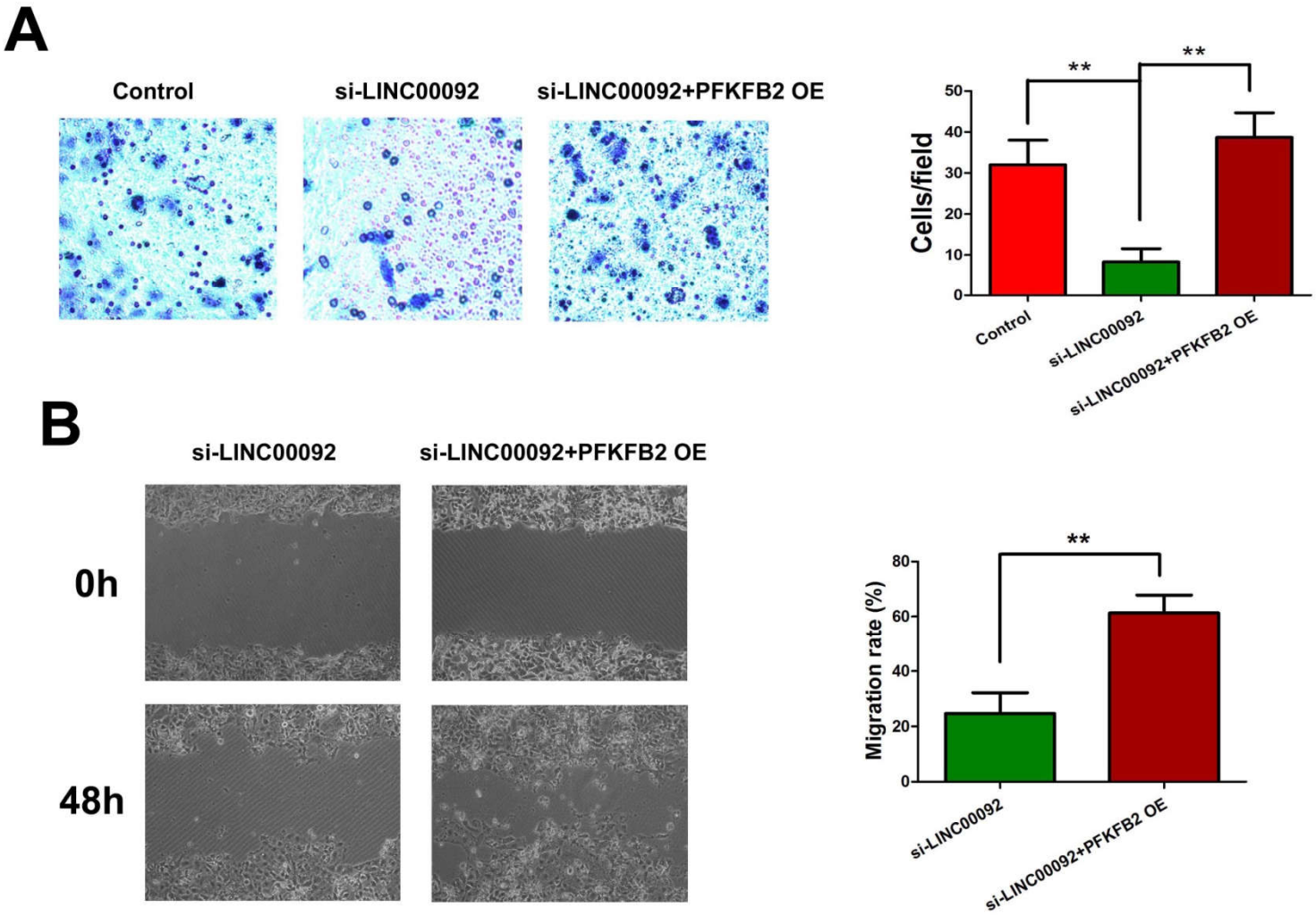


**Supplementary Figure 9. Enhanced LINC00092 expression in ovarian cancer cells could offset the metastasis-attenuating effects of CXCL14 knockdown in CAFs.** (A) Transwell assay for A2780s cells transfected with control, A2780s cells transfected with LINC00092 siRNA, and PFKFB2-overexpressing A2780s cells transfected with LINC00092 siRNA, respectively. (B) Wound healing analysis of A2780s cells transfected with LINC00092 siRNA and PFKFB2-overexpressing A2780s cells transfected with LINC00092 siRNA, respectively. *, $P < 0.05$; **, $P < 0.01$; ***, $P < 0.001$.

**Supplementary Figure 10**

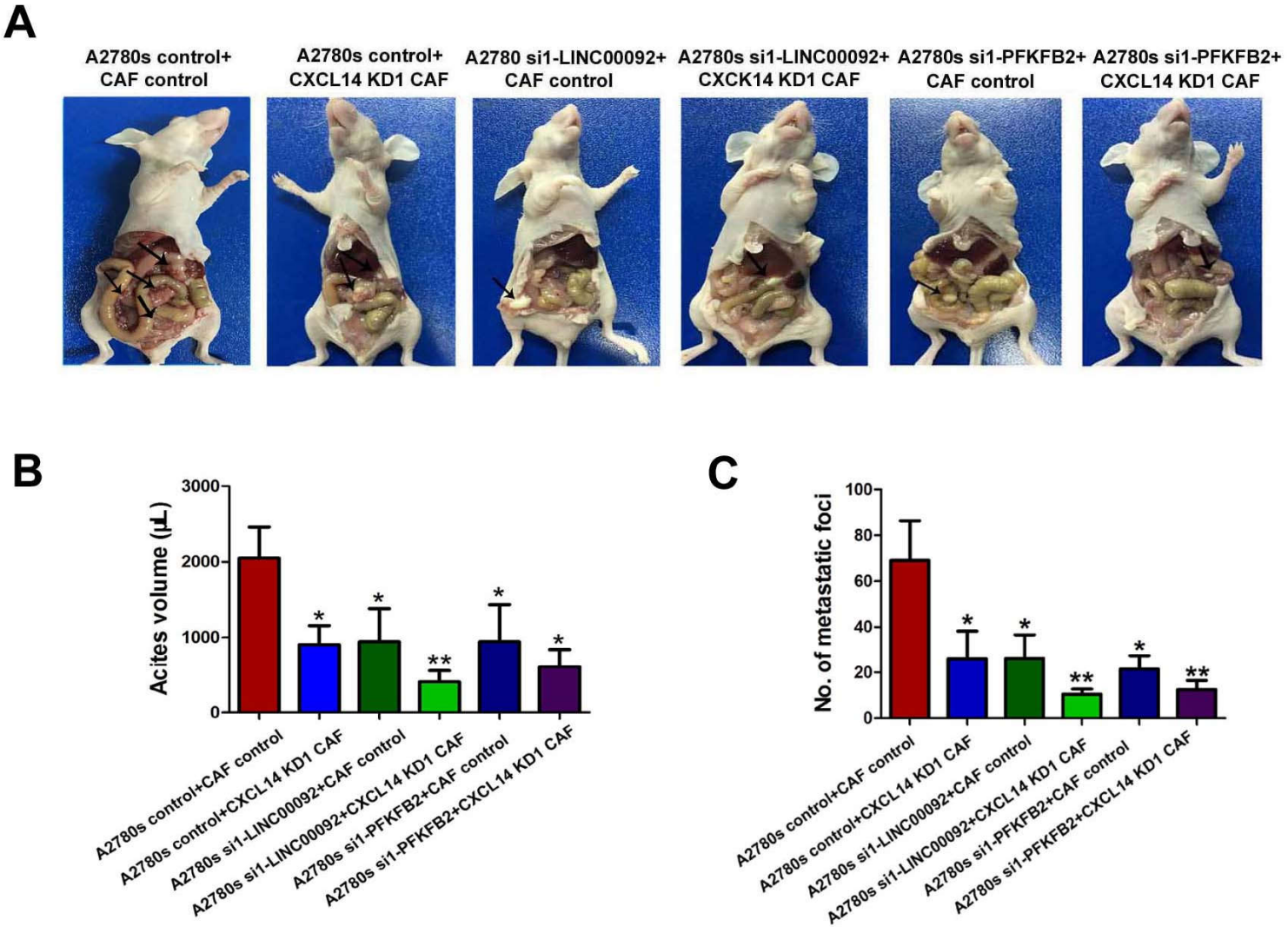


**Supplementary Figure 10. The necessity and sufficiency of CAF-secreted CXCL14, LINC00092 in ovarian cancer cells and PFKFB2 in ovarian cancer cells in the process of metastasis formation in ovarian cancer.** (A). Representative pictures of peritoneal metastasis in mice of each group indicated. (B) Box plot of the ascites volumes collected from the abdominal cavities of mice of each group indicated. (C) Box plot of number of metastatic nodules in the abdominal cavities of mice of each group indicated. *, $P < 0.05$; **, $P < 0.01$; ***, $P < 0.001$.

**Supplementary Figure 11**

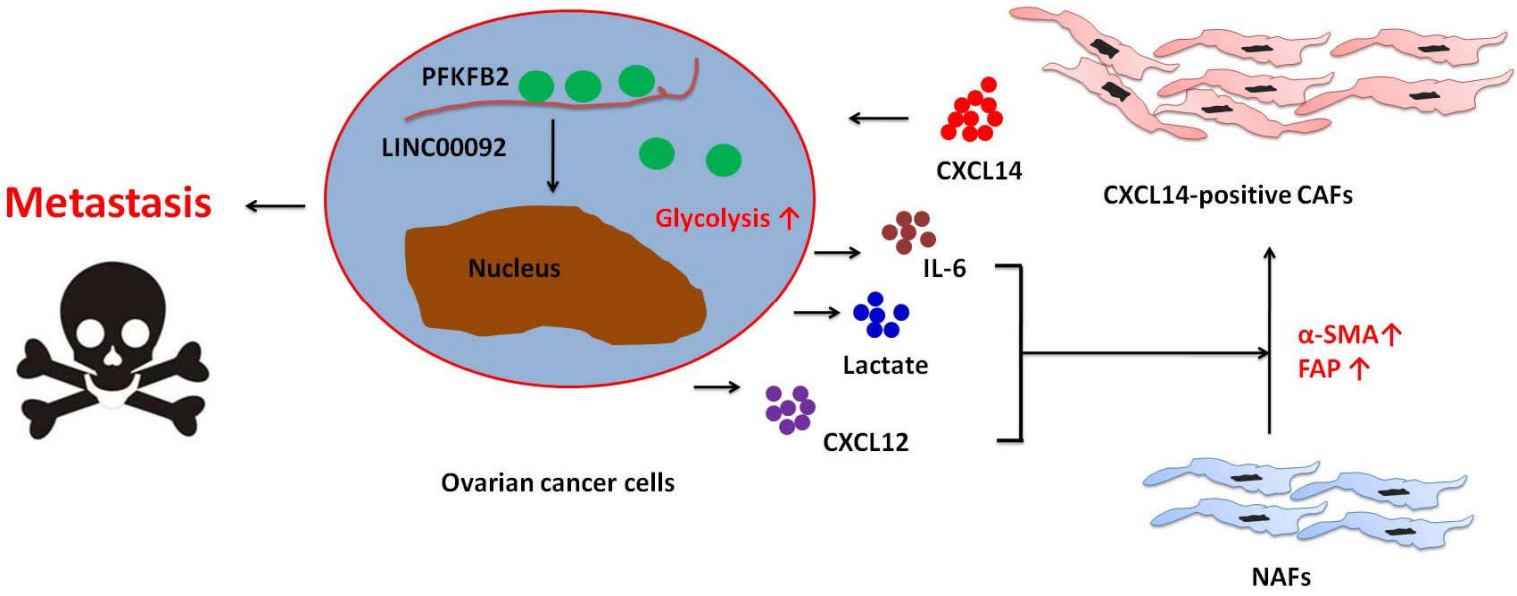


**Supplementary Figure 11. A schematic model summarizing the proposed mechanistic model of the a positive feedback loop between CXCL14-positive CAFs and ovarian cancer cells favorable for cancer metastasis by manipulating Warburg effect.**